Anthropogenic nitrogen deposition restructures decomposing microbial communities, altering SOM molecular composition, but not molecular complexity or diversity

Brooke E. Propson[1,2], William A. Argiroff[3], Grace A. Cagle[1], Rima A. Upchurch[3], Donald R. Zak[3,4], A. Stuart Grandy[5], and Zachary B. Freedman[1*]

[1]Department of Soil and Environmental Sciences
University of Wisconsin, Madison, WI, USA 53706
[2]University of Michigan Biological Station
9133 Biological Rd, Pellston, MI, USA 49769
[3]School for Environment and Sustainability
[4]Ecology and Evolutionary Biology
University of Michigan, Ann Arbor, MI, USA 48109
[5]Department of Natural Resources and the Environment
University of New Hampshire, Durham, NH, USA 03824

*Corresponding author: Zachary B. Freedman, zfreedman@wisc.edu (ORCID: 0000-0001-9160-7470)

Abstract

Soil organic matter (SOM) consists of diverse biochemical constituents, spanning a spectrum of chemical complexity, and the relative abundance of these substrates influences microbial metabolism and soil carbon persistence. However, mechanistic controls governing these processes and how they may be affected by environmental change remains incomplete. This study aims to assess (1) the molecular-level changes that occur across stages of root decomposition, from undecayed plant root litter to 1-year decomposed root litter, to mineral SOM and (2) how these changes are altered by anthropogenic nitrogen (N) deposition by using SOM biochemical and microbiome datasets and a long-term field experiment. N deposition did not significantly alter undecomposed or 1-year decomposed root litter, but did alter decomposing microbial communities and mineral SOM biochemical composition, specifically in lignin- and lipid-derived compounds. Taken together, this restructuring of microbial communities and alteration of SOM biochemistry likely contributed to the previously observed reduction in SOM decomposition.

Keywords: SOM, biochemistry, bacteria, fungi, py-GCMS, decomposition

1. Introduction

Soil organic matter (SOM) constitutes the largest terrestrial organic carbon reservoir, and altered SOM decomposition dynamics under fluctuating environmental conditions could intensify or mitigate impacts of climate change. Inputs from plants, through the deposition of above- and below-ground plant residues and the release of exudates from plant roots represents the largest organic matter input to soils[1,2]. Litter chemical composition, which is often estimated in terms of its nitrogen (N) or lignin contents[3,4], is regarded as one of the primary controls over decomposition rates and SOM accumulation and the fate of these inputs is governed by soil microbial activity[5–9]. In recent decades, there has been a shift from traditional theory of SOM chemical recalcitrance, where biochemically recalcitrant lignified material was thought to constitute the majority of SOM because of its theorized resistance to microbial decomposition[10,11], towards a continuum model of SOM complexity that proposes microbial-derived products as the primary constituents of SOM and the potential importance of molecular diversity in enabling SOM persistence[12–15].

Biochemical compounds that comprise litter exist across a spectrum of chemical complexity from simple to complex substrates and the relative abundance of these potential substrates for microbial metabolism can have consequences for the fate of C stored as mineral SOM[7,14,16]. When plant litter undergoes microbially mediated breakdown during decomposition, the resulting products will differ depending on the initial biochemical quality of the plant litter, as well as the composition of the microbial community decomposing that material[7,17]. The potential importance of biochemical complexity and diversity for SOM persistence lies in the different microbial requirements for metabolizing different biochemical compounds, both for compounds that are structurally dissimilar, as well as ones that are largely similar but may

62 exhibit minor differences, such as differences in the position of functional groups (for example,
63 *ortho*- versus *para*- benzoic acid)[15,18]. This rise in the acknowledgement and potential
64 importance of a higher resolution understanding of SOM is a deviation from the standard
65 practice in which compounds are typically grouped together as classes (e.g., lipids, etc.) that are
66 assumed to behave similarly through the decomposition process. This results in individual
67 compounds being grouped into classes that are inherently less refined. However, with the
68 conceptual move away from stable SOM largely consisting of recalcitrant material towards a
69 spectrum of which biochemical complexity and diversity enable SOM persistence, research has
70 shown that certain SOM biochemical constituents are resistant to decomposition despite being in
71 a compound class that was traditionally viewed as "labile" (ex: long-chain lipids)[19]. As such,
72 there is increasing emphasis on the potential importance of SOM molecular complexity and
73 diversity in driving SOM persistence[12,15,20–22]. Critically, there is a need to determine how this
74 proposed relationship between SOM molecular diversity and persistence responds to changing
75 climatic conditions[23].

76 To better understand how anthropogenic N deposition, a pervasive driver of global
77 environmental change, affects the cycling and storage of SOM, we conducted a 37-year field
78 experiment to simulate future rates of anthropogenic N deposition. After 20 years of
79 experimental N deposition inputs, we found that anthropogenic N deposition slowed the rate and
80 extent of organic matter decomposition, resulting in the accumulation of lignified material in
81 mineral soil derived primarily from fine root litter[24–26]. This change in SOM biochemistry in
82 response to N deposition was associated with decreases in lignolytic fungi and positively
83 associated with saprotrophic bacteria[24,27–29]. However, lignin, and its identifiable derivatives,
84 often comprises ≤10% mineral SOM[19,30–33], meaning a substantial majority of SOM

85 biochemistry has been considered unaltered by N deposition. A higher resolution analysis of
86 SOM chemistry (i.e., at the level of individual compounds) and the soil microbiome through
87 decomposition and N deposition remains a critical gap in our knowledge on the persistence of
88 SOM that built up under anthropogenic N deposition.

89 By using both broad (compound classes) and more refined (individual compounds) SOM
90 biochemical and soil microbiome datasets, in the context of a long-term field study, the primary
91 objective of this study was to assess the effect of experimental N deposition on the trajectory of
92 organic matter decomposition and stabilization from undecayed plant root litter to mineral SOM.
93 We assessed the effect of experimental N deposition on SOM molecular abundance, diversity,
94 and complexity during microbial decay by establishing a decomposition gradient from
95 undecomposed fine roots to mineral SOM. Here, we define SOM molecular diversity analogous
96 to species richness and evenness, where molecular richness represents individual biochemical
97 compound counts and molecular evenness describes their relative abundance. We define SOM
98 molecular complexity as how structurally (dis)similar biochemical compounds that constitute
99 SOM are to one another[34]. More molecularly complex SOM would thus have fewer structural
100 similarities between its compounds. We hypothesized that experimental N deposition will elicit
101 changes in organic matter biochemistry at the individual compound-level that are not detected
102 when assessed at the less refined compound class-level, and these compound substitutions may
103 have functional implications for storage of SOM in the system. We further hypothesized that
104 changes in SOM biochemistry will be associated with changes in microbial community
105 composition that can explain the observed biochemical changes. Finally, we hypothesize that
106 individual compound substitutions result in altered soil organic matter biochemical diversity and
107 molecular complexity, potentially leading to long-term changes in SOM persistence.

2. Methods

2.1. Description of study sites

The Michigan Nitrogen Deposition Gradient Study was established in 1987 to examine the effects of atmospheric N deposition on ecosystem biogeochemical processes. Spanning a 500-km distance, the study area in Michigan, USA, consists of four replicate sugar maple (*Acer saccharum*) dominated northern hardwood forest stands on sandy spodosol soil (Typic Haplorthods of the Kalkaska series). The stands contain a thick organic horizon that includes a mat of fine roots (Oe/Oa) at its boundary with the A horizon. The stands are floristically and edaphically matched and encompass the full latitudinal range of northern hardwood forests in eastern North America and the Upper Great Lakes Region[35], allowing us to generalize our findings across this widespread ecologically and economically important ecosystem (Table S1). At each site (n = 4), there are six 30-m by 30-m plots, three of which received experimental N additions (30 kg NO_3^-–N ha^{-1} yr^{-1}) in the form of $NaNO_3$ pellets applied annually in six equal applications throughout the growing season beginning in 1994 and three of which receive ambient atmospheric N deposition (Figure 1).

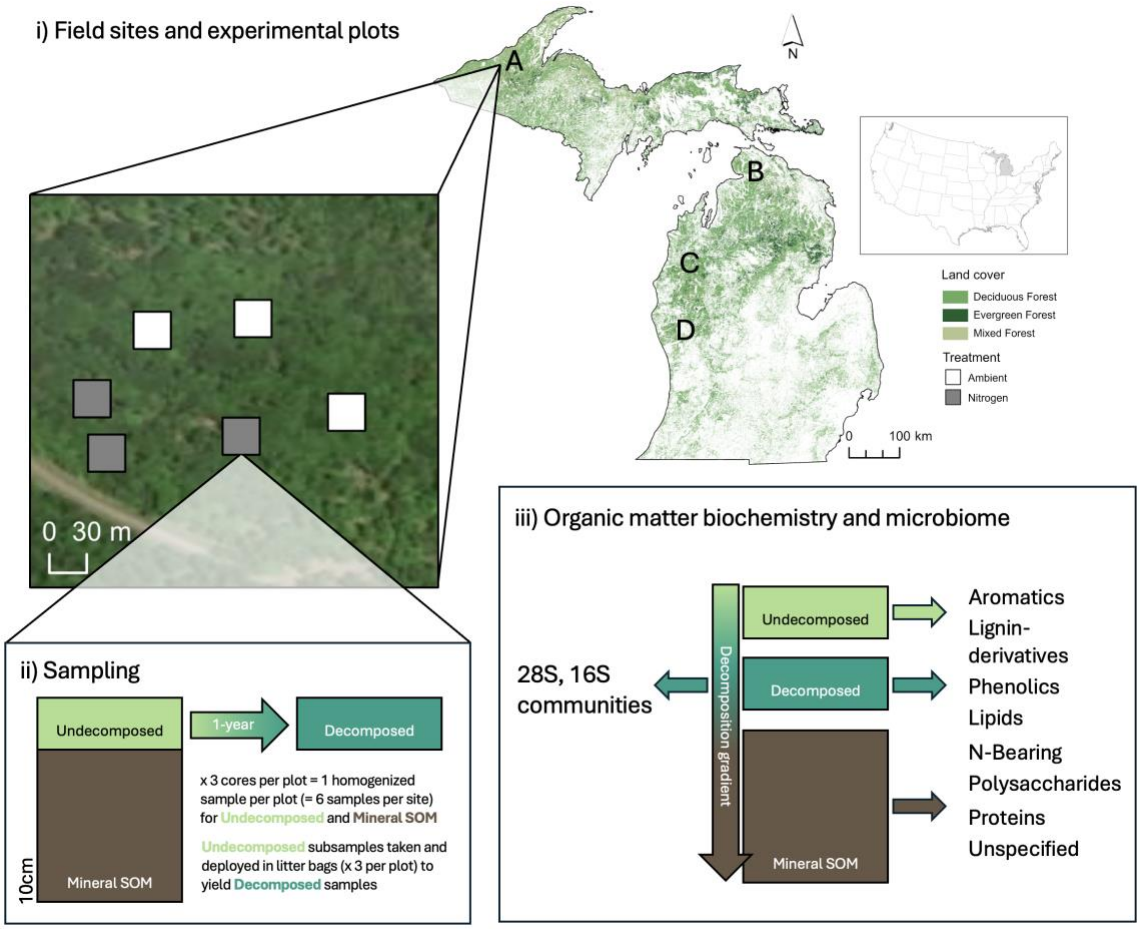

Figure 1. The distribution of study sites in Michigan, USA that span the geographic range of northern hardwood forests. At each site (n = 4), there are six 30 m x 30 m plots, three of which received annual experimental nitrogen (N) additions in the form of 30 kg NO_3^-N ha^{-1} yr^{-1} beginning in 1994 and three of which receive ambient atmospheric N deposition (i). Maps created using ArcGIS Pro: release 3.3.1[36]. Cores were collected (n = 3 per plot) to yield the undecomposed and mineral SOM samples. Subsets of undecomposed material were deployed in litter bags and left to decompose for 1-year to yield the decomposed samples (ii). The biochemistry of all three sample types was assessed using pyrolysis-GC/MS and bacterial and fungal community composition was determined on the decomposed samples (iii).

146 **2.2. Field-based experiment, sampling, and sample processing**

147 This experiment was designed to produce samples that constitute a gradient of fine root
148 decomposition, spanning undecomposed fine roots, 1-year decomposed fine roots, and more
149 highly decomposed mineral soil organic matter. To do this, samples were collected in September
150 and October 2013 by collecting soil cores to a depth of 10cm (5-cm-diameter), which included
151 both Oe/Oa and A horizons[24,37]. Cores were transported on ice to the University of Michigan and
152 stored at -20°C. Cores were thawed and passed through a 2mm sieve, and first- through third-
153 order fine roots were collected and pooled at the plot level[38,39]. Roots were rinsed to remove
154 mineral soil and dried at 60°C for 24 hours. The outcome of this processing yielded the
155 "undecomposed" and "mineral SOM" sample fractions (Figure 1). For this purpose, roots from
156 fresh Oe/Oa horizon samples are considered undecomposed in that relative to the other sample
157 types in this experiment, they have undergone decomposition to a lesser degree as indicated by a
158 light coloration and lack of observable decay. Organic material in the mineral soil represents
159 organic matter that has undergone the greatest degree of decomposition and exists as a relatively
160 stable form of SOM compared to organic horizon material[40].

161 To obtain the intermediate, "decomposed" samples, a subset of the undecomposed fine
162 roots from each plot were sterilized and placed in mesh litter bags, deployed in the field, and
163 collected after 12 months. Prior to field incubation, fine roots were sterilized to remove soil
164 microbes using ethylene oxide[41], a process that minimally alters organic matter biochemistry[42],
165 as compared to other methods such as autoclaving[43]. Sterilized fine roots (~2g dry weight) were
166 placed into 15x15cm mesh litter bags constructed with 300 µm polyester mesh on top and 20µm
167 polyester mesh on bottom to allow for microfauna and fungal hyphae to enter the bags[37,44]. Litter
168 bags were deployed in their respective plots to their original location in the soil profile at the

169 boundary of the Oe/Oa and A horizons (*n* = 3 litter bags/plot at 6 plots/site; *n* = 72 litter bags
170 total). Litter bags were placed in the field in June 2014 and collected in June 2015, immediately
171 storing each bag on ice. The contents of each litter bag were homogenized by hand and
172 composited at the plot level. The decomposed fine root samples were subsampled for
173 biochemical analyses, dried at 60°C for 24 hours, and the remaining decomposed fine root
174 material was stored at -80°C for microbial community analyses. Supporting justification and
175 additional details on sample collection and processing can be found in Argiroff et al. (2019)[24].

176 **2.3. Organic matter biochemistry**

177 Subsets of each of the three sample types (undecomposed fine roots, decomposed fine
178 roots, and mineral soil; herein referred to as three different stages of decomposition) were ground
179 with a ball mill and assessed for organic matter biochemistry using pyrolysis-GC/MS[45]. Samples
180 were pyrolyzed at 600°C in quartz tubes for 20 seconds using a DS Pyroprobe 5150 pyrolyzer
181 and analyzed using a ThermoTrace GC Ultra gas chromatograph (Thermo Fisher Scientific,
182 Walthan, MA, USA) and ITQ 900 mass spectrometer (Thermo Fisher Scientific)[24,46] at the
183 University of New Hampshire. Compound peaks were identified and assigned using the
184 Automated Mass Spectral Deconvolution and Identification Systems (AMDIS v2.65) software,
185 the National Institute of Standards and Technology (NIST) compounds library, and published
186 literature[13,45]. Organic matter compounds are expressed as the % relative abundance of total
187 sample peak area and classified at the individual compound-level and grouped by compound
188 source origin (e.g., lignin-derivatives, phenolics, aromatics, proteins, N-bearing, polysaccharides,
189 and lipids). Critically, individual compounds observed in pyrolysis-GC/MS analysis are
190 pyrolysis products of a source compound and are classified according to the nature of their
191 source compound. Identifiable compounds with potentially multiple or unknown origins were

192 classified as unspecified[13]. In total, this effort yielded 260 identifiable compounds, each assigned
193 to one of the 8 compound source classes described above (Figure 1). In this study, we refer to
194 analyses of individual pyrolysis-GC/MS compounds as "high-resolution" though we emphasize
195 that, in this context, high-resolution refers strictly to the increased molecular resolution and
196 biochemical information provided at the individual compound level as compared to at the
197 broader compound class level. High-resolution analysis in this context is therefore not referring
198 to the depth or analytical capabilities of pyrolysis-GC/MS itself relative to other high- and ultra-
199 high resolution mass spectrometry techniques, such as FTICR-MS, used in elucidating soil
200 organic matter biochemistry.

201 **2.4. Fungal and bacterial community composition**

202 Fungal and bacterial community composition was determined from the remaining subset of
203 decomposed root litter and characterized using ribosomal DNA sequence abundances.
204 Supporting justification and additional details on DNA isolation, PCR amplification, amplicon
205 sequencing, and sequence quality control can be found in Argiroff et al. (2019)[24]. Briefly, total
206 genomic DNA from three replicate subsamples taken from each litter bag was isolated using the
207 DNeasy Plant Mini Kit (Qiagen, Germantown, MD) and checked for quality with a NanoDrop
208 8000 Spectrophotometer (Thermo Scientific) and gel electrophoresis. Replicate extractions from
209 each litter bag were pooled and stored at -80°C prior to PCR amplification. PCR amplification
210 was performed using the LROR and LR3 primers[47] that target the D1-D2 region of the 28S
211 rRNA gene. The V1-V3 regions of the bacterial 16S rRNA gene were targeted using the primers
212 27f and 519r[48]. PCR products were purified using the MinElute PCR Purification Kit (Qiagen)
213 and the quality of the purified PCR products was assessed as described above. Sequencing was
214 performed at the University of Michigan DNA Sequencing Core on 16 SMRT chips with a

215 PacBio RS II system (Pacific Biosciences, Menlo Park, CA). Mean amplicon lengths were 688
216 bp for fungal 28S and 525 bp for bacterial 16S rRNA genes. Sequences were processed using
217 mothur v1.40.5[49]. Fungal sequences were aligned against a 28S reference alignment from the
218 RDP LSU training set[50] and bacterial sequences were aligned against the 16S SILVA v132
219 reference alignment[51]. Sequences were clustered into operational taxonomic units (OTUs) for
220 fungal and bacterial sequences at 99% and 97% sequence similarity, respectively. The most
221 abundant sequence for each OTU was used as the representative for that OTU, and taxonomic
222 assignments were made using the RDP classifier with the LSU training set v11 for fungi[52] and
223 the SILVA v132 reference alignment with the naïve Bayesian classifier[53] in mothur for bacteria.
224 Raw sequences are available in GenBank under the accession numbers SRR8591550 (16S) and
225 SRR8591551 (28S).

226 **2.5. Statistical Analyses**

227 To assess the effect of experimental N deposition on the trajectory of organic matter
228 biochemistry during decay, we assessed compositional changes elicited by the treatment in a
229 three-step approach at two increasing levels of biochemical resolution. At the least resolved
230 level, herein referred to as the compound class-level, we used two-way analysis of variance
231 (ANOVA) to test the effect of experimental N deposition, site, and their interaction on $\log_2$-
232 transformed compound class (n = 8) abundances for each of the three decomposition stages. At
233 the higher resolution level of analysis, herein referred to as the individual compound-level, we
234 performed PERMANOVA on Euclidean distance matrices of $\log_2$-transformed relative
235 abundances of individual compounds at the three decomposition stages testing for the effect of
236 decomposition stage, treatment, site, and their interactions on organic matter biochemistry. In the
237 case of a significant PERMANOVA outcome, we performed PERMDISP[54] to determine whether

238 this effect was driven by differences in composition, heterogenous variance (i.e., dispersion), or
239 both. The third step in our approach, at the individual compound-level, we additionally
240 performed differential abundance analysis (Wald test)[55,56] to test for the effect of N deposition on
241 individual compound abundances in decomposition stages with a significant PERMANOVA
242 treatment effect.

243 To assess how N deposition altered microbial community composition, we tested the
244 effects of experimental N deposition, site, and their interaction on bacterial, fungal, and
245 saprotroph community composition (as defined using FUNGuild in R)[57] using two-way
246 PERMANOVA and Bray-Curtis dissimilarity matrices calculated from Hellinger-transformed
247 bacterial phylum, fungal genus, and saprotrophic family abundances. We performed PERMDISP
248 to evaluate whether experimental N deposition (i.e., treatment) effects detected by
249 PERMANOVA were driven by true differences in community composition. To determine the
250 taxa that most differed in relative abundance across experimental N deposition, differential
251 abundance analysis was performed on the bacterial and fungal communities using DESeq2 with
252 *P*-value adjustment for multiple comparisons using the false discovery rate method[58,59]. To
253 assess how N deposition altered associations between microbial communities and organic matter
254 biochemistry, we performed Mantel tests on $\log_2$-transformed Euclidean distances of organic
255 matter biochemistry and Hellinger-transformed Bray-Curtis distances of bacterial, fungal, and
256 saprotroph communities. To determine whether changes in organic matter biochemistry were
257 associated with changes in microbial community composition elicited by experimental N
258 deposition, distance-based redundancy analysis (db-RDA) was performed.

259 We measured organic matter molecular diversity of each sample (n = 24 per
260 decomposition stage; 72 total) by calculating molecular species (i.e., individual compounds)

261 richness and evenness using the vegan package (v2.6.4)[60] in R and performed two-way ANOVA
262 to test the effect of decomposition stage, N deposition, and their interaction on each molecular
263 diversity metric. Molecular richness represents individual compound counts and molecular
264 evenness was determined by calculating Pielou's Eveness Index[61], which measures how equally
265 individual compound abundances are distributed within a sample. When applicable, pairwise
266 comparisons were made using Tukey's honest significant difference test (HSD) to control for
267 multiple comparisons. In contrast to molecular diversity, which assess the number of individual
268 compounds present (i.e., richness) and their distributions within a sample (i.e., evenness), we
269 define molecular complexity as a measure of how complex each individual compounds' physical
270 molecular structure is. To determine this, we calculated molecular complexity through two
271 approaches. First, using the chemodiv package (v0.3.0)[34] in R, we used molecular fingerprints
272 (PubChem Fingerprint) to quantify compound dissimilarities based on the structural properties of
273 the molecules[34]. The fingerprints were then used to calculate Jaccard dissimilarities between
274 compounds as a measure of their structural dissimilarity[34]. We created molecular structural
275 (dis)similarity networks to visually represent changes in organic matter molecular complexity
276 through decomposition and between the ambient and experimental N deposition treatment. Using
277 this method of visualization, more complex SOM would thus have fewer structural similarities
278 between compounds and depict a less connected network. In addition to the molecular structural
279 (dis)similarity networks, we computed molecular complexity values for each individual
280 compound using the Bertz/Hendrickson/Ihlenfeldt formula[62,63] computed by Cactvs 3.4.8.18
281 (PubChem release 2021.10.14)[64] and performed ANOVA to test the effect of N deposition on
282 molecular complexity. These values are estimates of how complicated an individual compound's

molecular structure is in terms of both the elements contained and structural symmetry and provide statistical significance to support network visualizations.

Due to the broad geographic expanse of our long-term field experiment and inherent heterogeneity of the soil environment, we accepted statistical significance at $\alpha = 0.1$[24,27,29]. All data processing, statistical analyses, and visualizations were performed and produced in R (v4.2.2)[65] and RStudio (version 2022.12.0+353)[66], relying extensively on R packages such as vegan (v2.6.4)[60], easyanova (v11.0)[67], and the tidyverse (v1.3.1)[68] packages.

3. Results

3.1 Compound class biochemistry

At the less-refined compound class-level, experimental N deposition significantly increased the relative abundance of lignin-derived compounds in the mineral SOM (+53%, $P = 0.09$; Figure S1; Table S2) across all sites. However, the experimental N deposition did not affect the abundance of any other compound class at any stage of decomposition (Table S3 and S4).

3.2 Individual compound biochemistry

When assessing the effect of experimental N deposition on the higher resolution, individual compound relative abundances across the three decomposition stages, the composition of individual compounds differed dependent on decomposition stage, site, and the N deposition treatment (decomposition stage × site × treatment; $F = 1.29$, $P = 0.05$; Figure 2; Table S5; Figure S2). Pairwise PERMANOVA at each decomposition stage revealed a significant effect of experimental N deposition on mineral SOM biochemistry ($F = 4.26$, $P = 0.004$; Figure 2; Figure S2), and no effect on the organic matter biochemistry at the undecomposed ($F = 0.18$, $P = 0.93$) or 1-yr decomposed ($F = 0.20$, $P = 0.92$) stages of decomposition (Table S5; Figure S2). Permutation tests of homogeneity of multivariate dispersion on the organic matter biochemistry

306 at each of the three decomposition stages were nonsignificant ($P > 0.1$; Table S6), indicating that
307 PERMANOVA detected differences in mineral SOM biochemical composition at the individual
308 compound-level between the ambient and experimental N deposition treatment, rather than
309 detecting changes in variability among samples (i.e., multivariate dispersion). Differential
310 abundance tests of individual compound abundances in mineral SOM revealed that experimental
311 N deposition led to the differential abundance of 19 out of 216 total compounds detected in the
312 mineral SOM (Figure 3). Of these differentially abundant compounds, 7 (3.2% of the total
313 number of compounds) were significantly more abundant in the N deposition treatment and 12
314 compounds (5.6% of total) were significantly more abundant in the ambient treatment (all $P \leq$
315 0.1; Table S7). Compounds more abundant under experimental N deposition compared to
316 ambient conditions included: phenol, 3-methyl- (aromatic combustion product), anthracene
317 (aromatic), 4-guaiacylpropane (lignin), benzeneacetic acid, 4-hydroxy-3-methoxy- (lignin),
318 benzene 1-methoxy-4-methyl- (lignin), n-decane (lipid), and 3-pyridinol (N-bearing).
319 Compounds more abundant in the ambient treatment included: benzene 1-ethenyl-4-methoxy-
320 (lignin), propene (lipid), isocrotonic acid (lipid), 3-methylpyridazine (N-bearing), ethanone, 1-(1-
321 methyl-1H-pyrrol-2-yl)- (N-bearing), 2,5-furandione, 3-methyl- (N-bearing), 2(5H)-furanone, 5-
322 methyl- (polysaccharide), 1,2-cyclohexanedione (polysaccharide), acetic anhydride
323 (polysaccharide), benzenepropanenitrile (protein), fluoranthene (unspecified), and (E)-1,3-
324 butadien-1-ol (unspecified).

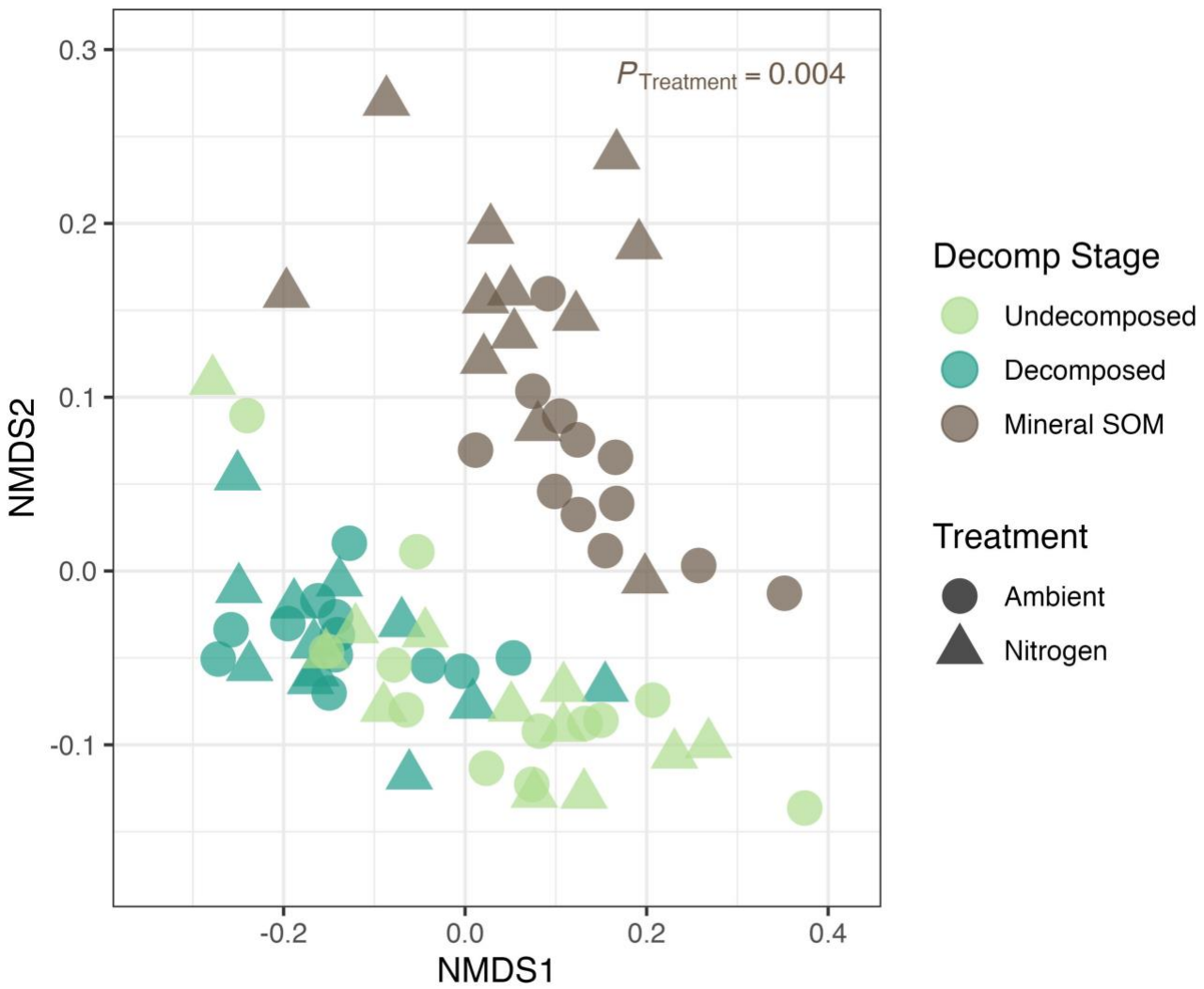

Figure 2. First two axes of non-metric multidimensional scaling (NMDS) ordination of Euclidean distances of $\log_2$ transformed py-GC/MS biochemical composition of individual samples (n = 72, k = 3, stress = 0.10). Data points represent the biochemical profile of each sample (n = 6 samples per site) and are colored by decomposition stage. The shape of the point represents if it received the ambient or the 30 kg NO_3^-–N ha^{-1} yr^{-1} nitrogen deposition treatment.

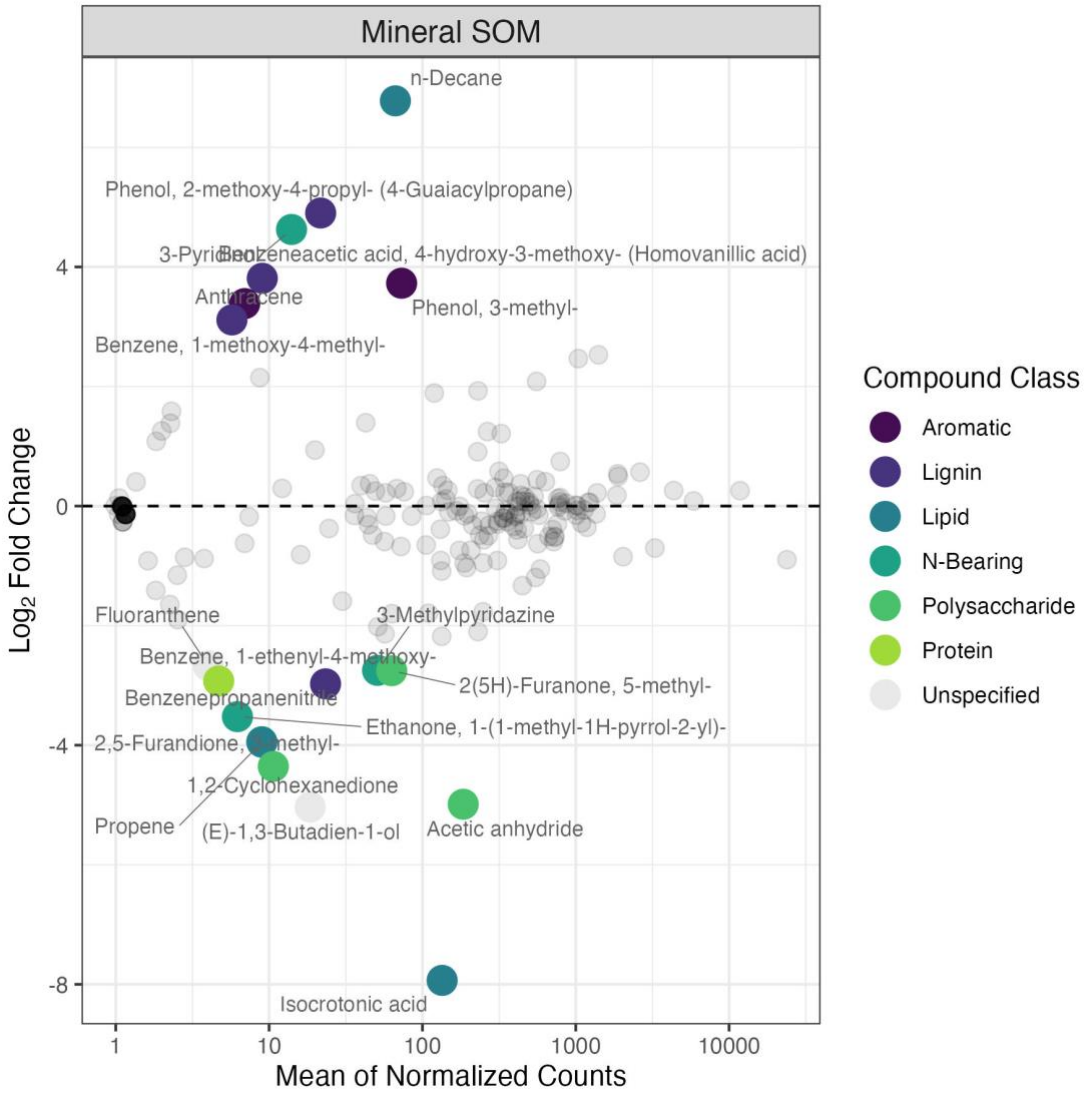

Figure 3. MA (Minus vs. Average) plot of mineral SOM py-GC/MS $\log_2$ fold changes of individual compound abundances between the ambient and nitrogen deposition treatments over the mean of normalized counts, calculated as the average normalized compound abundances taken across all samples. Compounds with a $P_{adj} < 0.1$ are colored by their compound source class. Colored compounds above the 0 line (represented by the black dashed line) indicate significantly higher abundance in the nitrogen deposition treatment, as compared to the ambient treatment, and vice versa for below the 0 line. See Table S7 for significant compound test statistics.

340 **3.3 Microbial community composition**

341 Experimental N deposition significantly altered bacterial (F = 3.20, *P* = 0.009), fungal (F
342 = 1.90, *P* = 0.017), and fungal saprotrophic community composition (F = 2.77, *P* = 0.006; Table
343 S8; Table S9). Permutation tests of homogeneity of multivariate dispersion on each community
344 were nonsignificant (*P* > 0.1; Table S10), indicating that PERMANOVA detected differences in
345 microbial community composition between the ambient and experimental N deposition treatment
346 for bacterial, fungal, and saprotrophic communities, rather than detecting changes in variability
347 among samples (i.e., multivariate dispersion). Specifically, using the Log_2 fold change approach
348 in DeSeq2, the abundances of 28 bacterial OTUs (1.6% of total OTUs) were significantly higher
349 under experimental N deposition as compared to the ambient treatment (Figure S3, Table S11).
350 These OTUs included members of the phylum Bacteroidetes (39%), Proteobacteria (29%),
351 Actinobacteria (14%), Patescibacteria (11%), and Armatimonadetes (7%). Under ambient
352 conditions, 13 bacterial OTUs (0.73% of total OTUs) were present in significantly greater
353 abundance. The phyla included Bacteroidetes (54%), Proteobacteria (38%), and Acidobacteria
354 (8%). The abundances of 14 fungal OTUs (2.6% of total OTUs) were significantly higher under
355 experimental N deposition as compared to the ambient treatment (Figure S3, Table S12). These
356 OTUs included members of the fungal classes Tremellomycetes (42%), Eurotiomycetes (17%),
357 Leotiomycetes (17%), Agaricomycetes (8%), Dothideomycetes (8%), and Sordariomycetes
358 (8%). Under ambient conditions, 2 fungal OTUs (0.43% of total OTUs) were present in
359 significantly greater abundance as compared to the N deposition treatment. The fungal classes
360 include Agaricomycetes (50%) and Sordariomycetes (50%). However, the composition of
361 bacterial (F = 1.70; P = 0.06) and fungal communities (F = 2.88; *P* < 0.001) differed among sites
362 (Table S8; Table S9) and the effect of experimental N deposition on bacterial and fungal

363 communities was not uniform across sites (site × treatment $P \leq 0.1$; Table S8). Specifically,
364 experimental N deposition did not elicit significant differences in bacterial community
365 composition at site B (F = 2.65; $P = 0.20$) or fungal community composition at site D (F = 1.00;
366 $P = 0.30$; Table S9).

367 **3.4 Microbial community associations with SOM biochemistry**

368 Fungal and bacterial communities were differentially associated with organic matter
369 biochemistry at the three decomposition stages in the ambient and N deposition treatments
370 (Figure S4). In the ambient treatment, bacterial community composition was significantly
371 correlated with organic matter biochemistry in the undecomposed root litter (R = 0.29, $P = 0.07$)
372 and weakly associated in the mineral SOM (R = 0.26, $P = 0.12$) but exhibited no relationship
373 with the organic matter biochemistry in the 1-yr decomposed root litter (Table S13). Under
374 experimental N deposition, bacterial community composition and organic matter biochemistry
375 were not correlated at any of the three decomposition stages. In the ambient treatment, fungal
376 community composition was also not correlated with the 1-yr decomposed root litter (Table S13)
377 and was significantly correlated with the organic matter biochemistry in the mineral SOM (R =
378 0.20, $P = 0.09$). Under experimental N deposition, fungal community composition was
379 significantly correlated with the 1-yr decomposed root litter biochemistry (R = 0.23, $P = 0.04$)
380 and marginally associated in the mineral SOM (R = 0.17, $P = 0.11$) but exhibited no relationship
381 with the organic matter biochemistry in the undecomposed root litter (Figure S4; Table S13). In
382 the ambient treatment, saprotroph community composition was marginally associated with
383 organic matter biochemistry in the undecomposed root litter (R = 0.18, $P = 0.15$) and
384 significantly correlated with the mineral SOM (R = 0.30, $P = 0.06$) but exhibited no relationship
385 with the organic matter biochemistry in the 1-yr decomposed root litter (Figure S4; Table S13).

386 Under experimental N deposition, saprotroph community composition and organic matter
387 biochemistry were not correlated at any of the three decomposition stages.
388 To directly link changes in organic matter biochemistry with changes in microbial
389 community composition elicited by experimental N deposition, we fit vectors for mineral SOM
390 individual compound abundances to bacterial ($R^2 = 0.27$; $P = 0.001$), fungal ($R^2 = 0.10$; $P =$
391 0.09), and saprotrophic ($R^2 = 0.27$; $P = 0.001$) distance-based redundancy analysis (db-RDA)
392 ordinations (Figure 4). Mineral SOM individual compound abundances were selected given the
393 observed differences in organic matter biochemistry in the mineral SOM in response to
394 experimental N deposition (Figure 2; Table S5; Figure 3; Table S7). The shift in bacterial
395 community composition driven by experimental N deposition (F = 3.20, $P = 0.009$) was
396 associated with shifts in the abundance of 28 compounds in mineral SOM (Figure 4; Table S14).
397 The three most represented compound classes include lignin ($n = 10$; 35.7%), unspecified ($n = 7$;
398 25.0%), and lipids ($n = 3$; 10.7%). The longest vectors include Pyrazolo[5,1-
399 c][1,2,4]benzotriazin-8-ol (N-bearing; vector length = 0.698), Phenol, 2,6-dimethoxy-4-(2-
400 propenyl)- (Methoxyeugenol) (lignin; length = 0.649), Benzene, 1,4-dimethoxy- (phenol; length
401 = 0.604), and Benzeneacetic acid, 4-hydroxy-3-methoxy- (Homovanillic acid) (lignin; length =
402 0.599). The shift in fungal community composition driven by experimental N deposition (F =
403 1.90, $P = 0.017$) was associated with shifts in the abundance of 42 compounds in mineral SOM
404 (Figure 4; Table S15). The three most represented compound classes include lignin ($n = 10$;
405 23.8%), unspecified ($n = 9$; 21.4%), and lipids ($n = 8$; 19.1%). The longest vectors include
406 Phenol, 2,6-dimethoxy-4-(2-propenyl)- (Methoxyeugenol) (lignin; length = 1.370), Ethanone, 1-
407 (3,4-dimethoxyphenyl)- (lignin; length = 1.268), Benzoic acid, 4-hydroxy-3,5-dimethoxy-,
408 hydrazide (unspecified; length = 1.262), and Ethanone, 1-(4-hydroxy-3,5-dimethoxyphenyl)-

409 (Acetosyringone) (lignin; length = 1.186). The shift in saprotrophic fungal community
410 composition under experimental N deposition (F = 2.77, P = 0.006) was associated with shifts in
411 the abundance of 21 compounds in mineral SOM (Figure 4; Table S16). The three most
412 represented compound classes include lignin (n = 7; 33.3%), unspecified (n = 7; 33.3%), and N-
413 bearing (n = 3; 14.3%). The longest vectors include Trimethylphenol (unspecified; length =
414 1.370), Ethanone, 1-(4-hydroxy-3,5-dimethoxyphenyl)- (Acetosyringone) (lignin; length =
415 1.360), n-Decane (lipid; 1.350), and Benzoic acid, 4-hydroxy-3,5-dimethoxy-, hydrazide
416 (unspecified; 1.350).

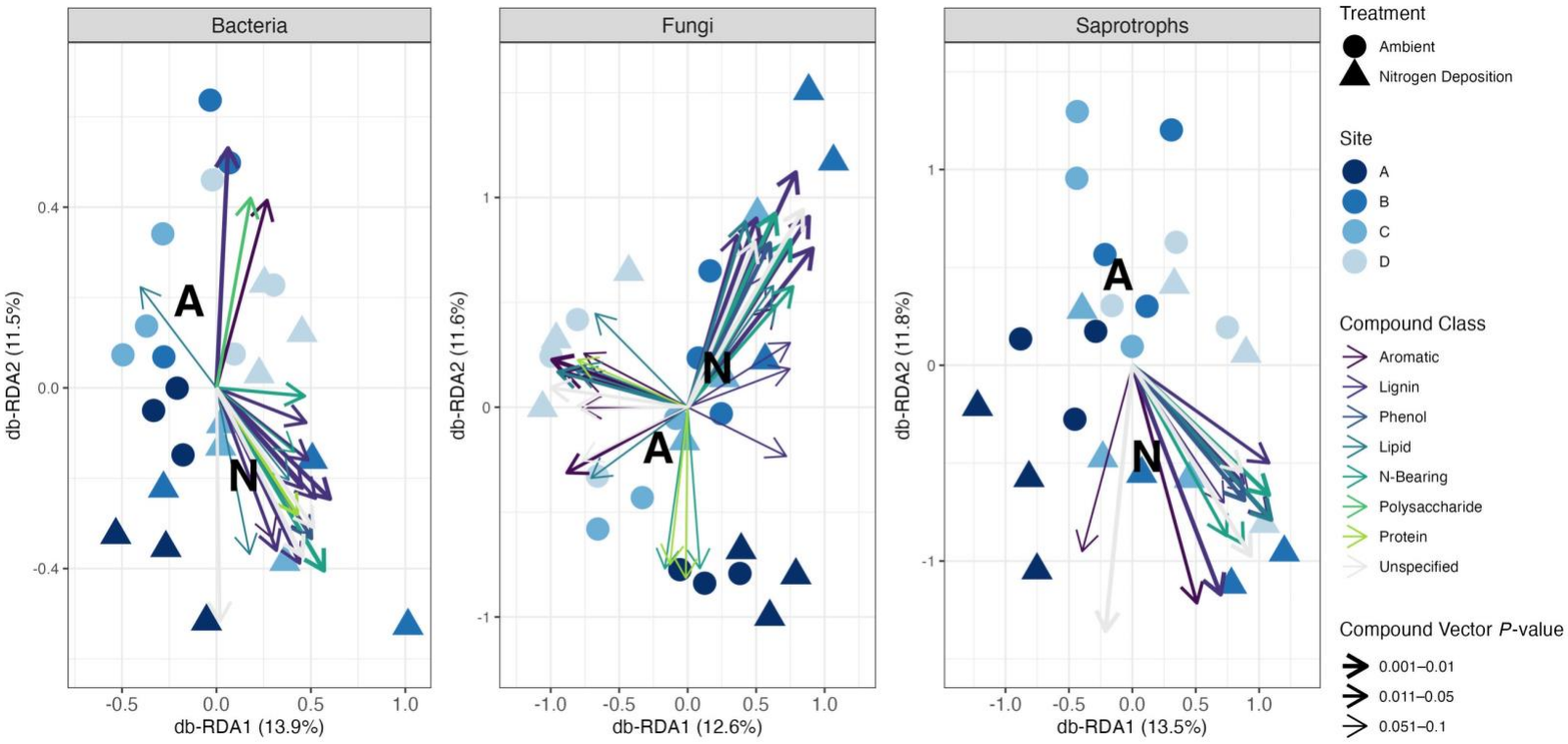

Figure 4. Biplots of distance-based redundancy analysis (db-RDA) ordinations of bacterial phyla, fungal genera, and saprotrophic families (points) and SOM compounds (vectors). The db-RDA was performed on Bray-Curtis dissimilarity matrices calculated from Hellinger-transformed taxon abundances. Ordinations were constrained by experimental N deposition and site, which together accounted for 31.8% of variation in Bray-Curtis dissimilarity for bacteria, 38.1% for fungi, and 33.3% for saprotrophs. Points represent individual samples (n = 6 samples per site) and are colored by site. Point shape indicates nitrogen treatment (ambient or 30 kg NO_3^-—N ha^{-1} yr^{-1} deposition). Treatment centroids are shown in black as "A" (ambient) or "N" (nitrogen deposition). Vectors represent mineral SOM compounds fitted to the ordination. Compounds with goodness of fit P-values ≤ 0.1 are displayed and are colored by their source compound class.

3.5 Biochemical diversity and complexity

Experimental N deposition did not affect molecular species richness (F = 0, $P = 0.97$) or evenness (F = 0.39, $P = 0.53$) at any of the three decomposition stages (Figure 5; Table S17). Given the observed treatment differences in biochemical composition in the mineral SOM only, we assessed the effect of experimental N deposition on molecular complexity at only the mineral SOM decomposition stage. To determine how experimental N deposition affects molecular complexity (i.e., how structurally similar compounds that constitute SOM are to one another), compound co-occurrence and structural dissimilarity matrices were generated for mineral SOM biochemistry in both treatments. Under ambient conditions in the mineral SOM, molecular network analysis revealed 197 nodes, representing compounds, and 2450 edges, representing the structural similarities present between those compounds (Figure 6). Molecular network analysis of the mineral SOM biochemistry in experimental N deposition revealed it did not significantly alter the number of compounds present ($n_{\text{nodes}} = 187$) nor the structural similarities between compounds ($n_{\text{edges}} = 2502$; Figure 6). Molecular complexity values calculated using the Bertz/Hendrickson/Ihlenfeldt formula affirmed that the N deposition treatment did not significantly alter individual compound molecular complexity in the mineral SOM (F = 0, $P = 0.997$; Figure S5).

Decomposition stage had a significant effect on molecular richness (F = 9.49, $P<0.001$) and evenness (F = 12.22, $P<0.001$; Figure 5; Table S17). HSD-adjusted pairwise comparisons revealed significantly higher molecular richness at the 1-yr decomposed stage compared to the undecomposed (post hoc $P = 0.001$) and mineral SOM (post hoc $P<0.001$; Figure 5; Table S18). Molecular evenness was significantly higher in the 1-yr decomposed (post hoc $P = 0.002$) and mineral SOM (post hoc $P<0.001$) stages of decomposition as compared to the undecomposed

root litter (Figure 5; Table S18). There was no difference in molecular evenness between the 1-yr decomposed and mineral SOM decomposition stages (post hoc $P = 0.39$; Figure 5; Table S18). In the undecomposed root litter, molecular network analysis revealed 209 nodes and 2095 edges, while the 1-yr decomposed root litter network had 225 nodes and 3372 edges, and the mineral SOM network had 216 nodes and 3022 edges (Figure S6). Molecular complexity values calculated using the Bertz/Hendrickson/Ihlenfeldt formula affirmed that decomposition stage did not significantly alter individual compound molecular complexity at any point ($F = 0.01$, $P = 0.99$, Figure S7).

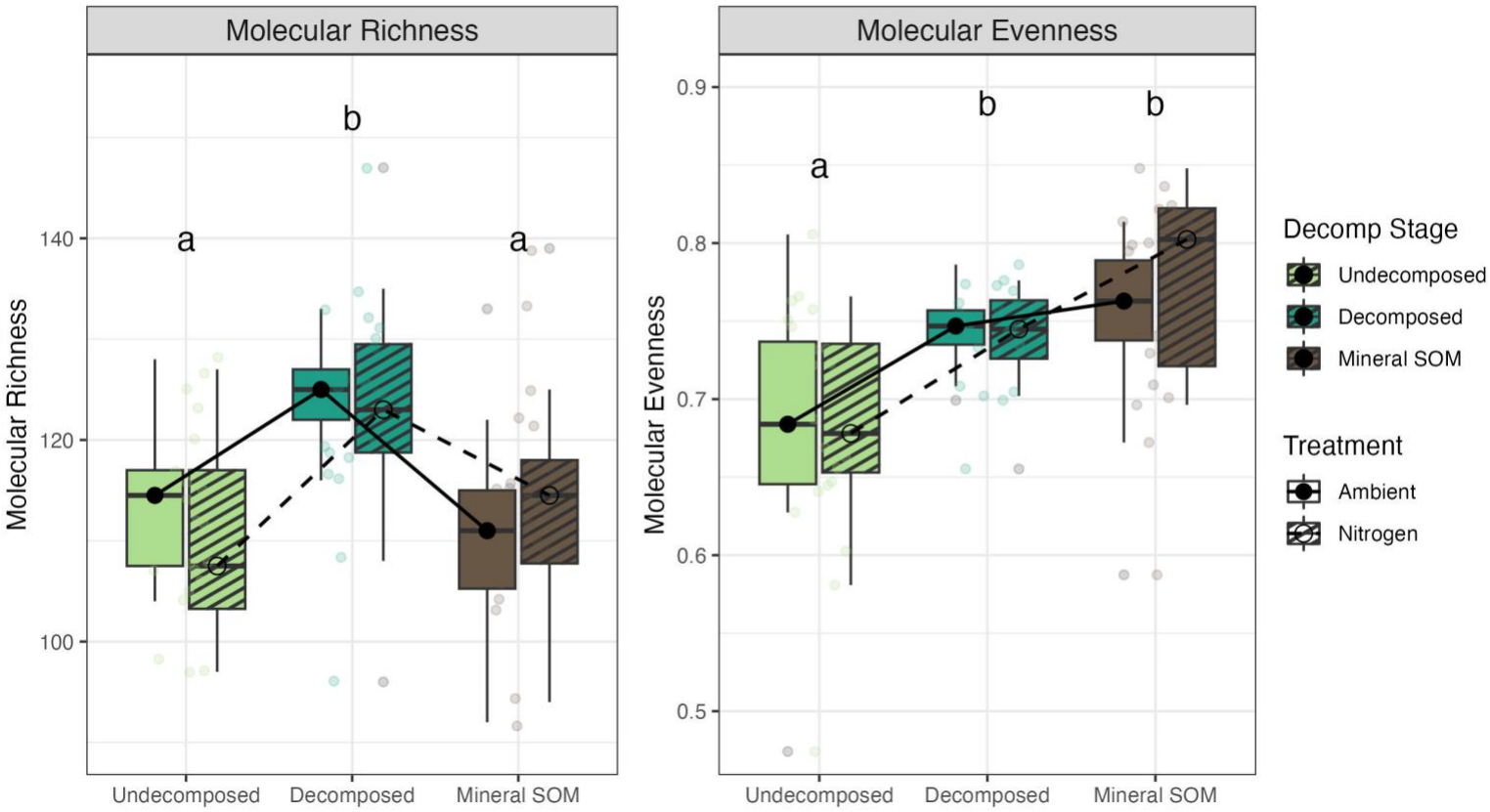

Figure 5. The effect of the nitrogen deposition treatment and decomposition stage on molecular richness (left) and evenness (right). Within each figure, ambient values are displayed on the left (solid) and nitrogen deposition treatment values are displayed on the right (dashed) for each decomposition stage (n = 3). Individual sample values (n = 72) are displayed. Two-way ANOVA was used to test the effect of Decomposition Stage, Treatment, and Decomposition Stage x Treatment interaction. The effect of Decomposition Stage was significant for both richness (F_{decomp} = 9.49, P<0.001) and evenness (F_{decomp} = 12.22, P<0.001). Decomposition Stage pairwise comparisons (Tukey's HSD) are displayed as letters (see Supplementary Table S18).

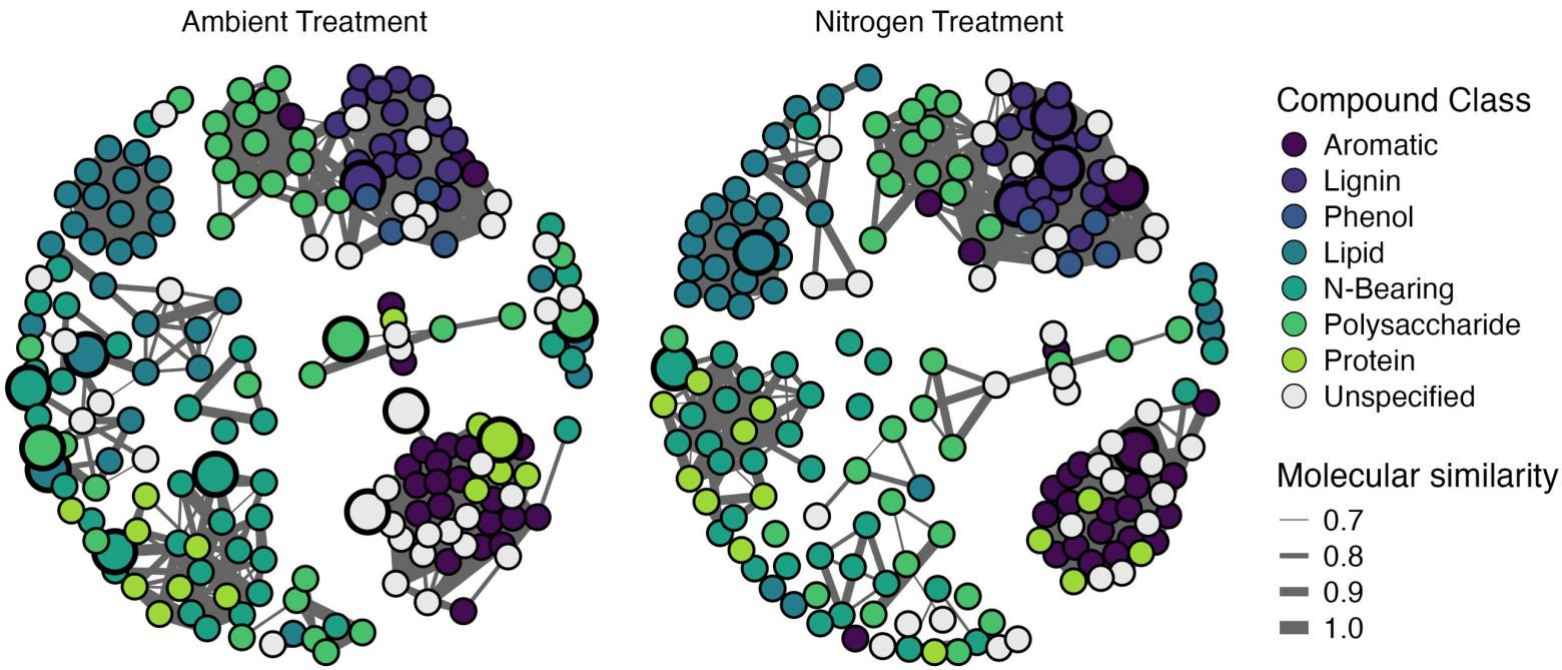

Figure 6. Molecular networks showing relationships between the biochemical compounds present in the mineral SOM under ambient (left) and nitrogen deposition (right) conditions. Nodes represent individual molecules (ambient: n = 197; nitrogen treatment: n = 189) and edges represent the quantity of interactions and relationships between those molecules (ambient: n = 2450; nitrogen treatment: n = 2502). Thickness of the edges was determined by the molecular similarity with a cut off value of 0.7. Nodes are colored by the compound class to which that individual molecule belongs. Enlarged nodes represent the molecules in greater abundance in each respective treatment derived from differential abundance analysis (Figure 3; Table S7).

4. Discussion

High resolution molecular analyses reveal N deposition elicits changes to SOM biochemistry that were previously undetectable, supporting our first hypothesis. It is common to assess SOM biochemistry by grouping individual biochemical compounds into broader classes, such as lipids or lignin-derived compounds, as a means to simplify biochemical heterogeneity and diversity by grouping compounds that are suspected to behave similarly based on the relative similarity of their structure or other physical properties or factors[12,13,24,69,70]. In doing so, the abundances of individual compounds within a compound class are combined, leading to a loss in the potential resolution of SOM biochemical information, and potentially making impacts of environmental change on SOM biochemical constituents undetectable. As the resolution at which we can examine SOM biochemistry has increased with technological advances, so has the importance of identifying and elucidating the complexity within these traditional compound classes. While it has been common to assume that individual compounds within a class of compounds behave uniformly, there is increasing evidence for contrasting and compounding origins within a compound class and the different potential pathways of mineralization will have implications for the formation and persistence of mineral SOM[2,7,19,20]. As such, the implementation of more refined analytical analyses (i.e., high[er] resolution) that aid in elucidating these molecular-level differences can increase understanding of mechanisms governing SOM persistence; a necessary step toward increasing organic matter in soil as a viable climate change mitigation strategy[15,20].

To demonstrate this assertion, previous research efforts in this long-term field experiment have detected increases in lignin-derived compounds in mineral SOM under experimental N deposition, with no detectable changes to other components of mineral SOM biochemistry[24,25].

However, high resolution analysis used in this study revealed numerous individual compounds changed in mineral SOM within multiple additional compound classes in response to experimental N deposition that may have consequences for the processes of organic matter decay and soil C storage (Figure 3; Table S7). For example, the abundance of lipids in mineral SOM exhibited no effect of experimental N deposition at the compound class-level (Figure S1; Table S2). However, at the individual compound-level, in the ambient treatment, two molecules that are produced from the combustion of lipids (propene and isocrotonic acid) were 15-times and over 200-times more abundant, respectively, compared to the experimental N deposition treatment (Figure 3; Table S7). Whereas under experimental N deposition, one lipid molecule (n-decane) was over 100-times more abundant compared to in the ambient treatment (Figure 3; Table S7) and was one of the most significant compounds associated with the shift in saprotrophic community composition driven by experimental N deposition (Figure 4; Table S16). This reorganization of individual compounds within compound classes is undetectable by less refined analysis, ultimately leading to no observable effect of experimental N deposition on the abundance of lipids as a class of compounds (Figure S1; Table S2), but is critical for understanding the fate of these substrates in SOM. Lipids are a highly heterogenous class of compounds with significant input from both plants and soil microbes[71,72]. Though there is rising evidence that stable mineral SOM is largely microbial-derived, it remains unclear and highly context dependent how much is plant-derived[13,19,20,73–76]. Thus, it is likely that observed changes in the microbial community can account for a portion of the variance observed in SOM lipid biochemistry, supporting our second hypothesis. Microbial taxa that are relatively more abundant under experimental N deposition and exhibit fast growing (i.e., copiotrophic) traits may contribute to increased lipid signatures in mineral SOM through enhanced turnover, resulting in

521 necromass production. In this study, members of the phyla Bacteroidetes and Acidobacteria, and
522 the genus *Paraburkholderia* were in significantly greater abundance under experimental N
523 deposition compared to the ambient treatment (Figure S3), all of which harbor taxa that exhibit
524 copiotrophic characteristics[77,78]. However, estimations of microbial necromass C in forest soils
525 suggest that a substantial portion (~70%) of C in persistent SOM could be plant-derived[79,80], and
526 that the contribution of plant-derived lipids to this C pool can be greater than that of lignin[20]. All
527 three of the differentially abundant lipid molecules across the ambient and experimental N
528 deposition treatments are involved in both plant and microbial metabolic processes[81–83]. As such,
529 more detailed knowledge of the specific metabolic reactions, which plants or microbes are
530 producing them, and how these compounds end up in mineral SOM is necessary to understand
531 the longevity of these substrates in the system[84].

532 Proteins and other N-containing compounds exhibited similar trends at these differing
533 analytical scales. Despite no statistical difference in the abundance of proteins at the compound
534 class-level, at the individual compound-level one protein molecule (benzenepropanenitrile) was
535 almost 8-times more abundant in the ambient treatment compared under experimental N
536 deposition (Figure 3; Table S7). The hydrolysis of benzenepropanenitrile (i.e., 3-
537 phenylpropionitrile) is catalyzed by the nitrilase enzyme (EC 3.5.5.1)[85–88], yielding a carboxylic
538 acid and ammonium (NH_4^+). The gene which encodes the enzyme that ultimately carries out this
539 reaction is found in the genomes of two soil bacteria, one of which being *Paraburkholderia*
540 *phymatum*[86,89–92]. In this study, *Paraburkholderia spp.* (n = 3; Table S11) were in significantly
541 greater abundance under experimental N deposition compared to the ambient treatment (Figure
542 S3). *Paraburkholderia spp*. are known decomposers in forests, particularly sugar maple forests
543 like the ones in this study[93]. Thus, it is plausible that increased enzymatic activity produced by

544 *Paraburkholderia spp.* under experimental N deposition catalyzed this reaction, leading to
545 significantly lower benzenepropanenitrile abundance in the N deposition treatment. These
546 findings suggest that changes to microbial community composition in response to environmental
547 stimuli may have functional consequences and elicit changes to the biochemical composition of
548 organic matter that eventually becomes stable mineral SOM.

549 In addition to the novel findings detailed above, high resolution analysis of SOM
550 biochemistry revealed additional compositional insight into lignin dynamics in response to the
551 experimental N deposition that may underlie resistance to microbial decomposition, further
552 supporting our first hypothesis. Previous work in this long-term experiment showed that
553 anthropogenic N deposition slowed the rate and extent of organic matter decomposition,
554 ultimately resulting in the accumulation of lignified material in mineral SOM under experimental
555 N deposition (+53%, $P = 0.09$; Figure S1; Table S2)[24–26,29]. However, at the individual
556 compound-level, changes in the composition of lignin compounds in mineral SOM were detected
557 under both ambient and experimental N deposition conditions. In the ambient treatment, one
558 lignin-derived molecule (benzene, 1-ethenyl-4-methoxy-) was almost 8-times more abundant
559 compared to under experimental N deposition (Figure 3; Table S7). Whereas under experimental
560 N deposition, three different lignin-derived molecules (benzene, 1-methoxy-4-methyl-,
561 homovanillic acid, and 4-guaiacylpropane) were 8-times, 14-times, and 29-times more abundant
562 than in the ambient treatment, respectively, ultimately leading to the overall increase observed at
563 the compound class-level (Figure 3; Figure S1; Table S7).

564 At the relatively less-refined compound class-level, it is not possible to detect this
565 reorganization of different lignin molecules, as observed here, that ultimately affects the
566 interpretability of the stability of the compound class as a whole. Lignin is a complex

macromolecule that is highly variable in terms of its primary structure. Which lignin monomers and functional groups are present, in what quantities, and what linkages connect them affect the decomposability of lignin polymers by soil microbes[94–97]. For example, lignin polymers containing higher quantities of monomers of the guaiacyl (G) subunit are more resistant to decomposition, resulting in significantly lower mass loss, than lignin polymers composed of other subunits[16,96]. The 29-times greater abundance of 4-guaiacylpropane and 14-times greater abundance of homovanillic acid, a G subunit decomposition product[98], under experimental N deposition suggests that the SOM that has accumulated under anthropogenic N deposition is particularly compositionally resistant to microbial decomposition in terms of its lignin content. Thus, it is plausible that in this system, differences in the quality of lignin, in addition to the increases in lignin quantity[24], may be a factor contributing to the increased SOM observed under high N deposition conditions. This possibility has been suggested from earlier modeling studies in this system[26], and this is the first experimental observation to support this modeled result.

Differences in the composition of decomposing microbial communities observed under experimental N deposition support the claim that lignin in mineral SOM under increased anthropogenic N deposition is particularly resistant to decomposition or is simply not being metabolized by the microbial community in this treatment, further supporting our second hypothesis. While fungi are widely considered as primary lignin decomposers, evidence has shown that bacteria may play a non-inconsequential role in lignin decay[99,100]. Of the bacterial OTUs in higher abundance under N deposition conditions, just under half (43%) belong to the phyla Proteobacteria and Actinobacteria (Figure S3; Table S11). This finding aligns with previous work in this system that observed an increase in the abundance of bacteria associated with lignin decay under experimental N deposition[27,28]. The majority of lignin-degrading bacteria

identified to date represent three bacterial classes, all of which are within the Proteobacteria and Actinobacteria phyla: Actinomycetes, α-Proteobacteria, and γ-Proteobacteria[101–103]. Such bacteria capable of lignin degradation do so in an incomplete manner, such that smaller aromatic lignin-derived compounds are produced[104–106]. For example, bacterial species belonging to the class γ-Proteobacteria produce the intermediate phenolic compound homovanillic acid during plant litter and lignin decomposition[107]. In this study, homovanillic acid was one of the most significant compounds associated with the shift in bacterial community composition driven by experimental N deposition (Figure 4; Table S14) and was in significantly higher abundance in the N deposition treatment compared to the ambient treatment (Figure 3; Table S7). Additionally, benzoic acid, 4-hydroxy-3,5-dimethoxy-, hydrazide, a decomposition derivative of syringic acid, which is a key intermediate of bacterial catabolism of lignin compounds[108], was one of the most significant compounds associated with the shifts in fungal and saprotrophic community composition driven by experimental N deposition (Figure 4; Table S15; Table S16). Taken together, it is plausible that the accumulation of decomposition resistant lignin material under experimental N deposition was due, in part, to the incomplete bacterial metabolism of lignin and the inability to break down these compounds specifically.

Further, both bacterial and saprotrophic fungal communities exhibit strong relationships with the biochemistry of the organic matter in the undecomposed litter and mineral SOM under ambient conditions (Figure S4; Table S13). Yet, under experimental N deposition these relationships are lost. The expression of microbial genes and the subsequent production of extracellular enzymes that govern the breakdown of SOM are highly sensitive to N additions[29,109–112]. Under high N conditions, genes responsible for the production of extracellular enzymes that break down complex macromolecules, such as lignin, are downregulated[29].

613 Additional studies have observed a shift in microbial community composition under N
614 deposition conditions towards a community whose primary niche is the decay of simpler
615 compounds, such as cellulose[109,113,114]. Taken together, it is plausible that when N is readily
616 available, microbes do not need to expend the energy producing extracellular enzymes to break
617 down organic material and this decreased activity may result in a shift in the community
618 composition. The lack of microbial activity observed in previous studies, in consideration with
619 SOM biochemical relationships to microbial taxa observed here, may explain why we observed a
620 decoupling of SOM biochemistry and microbial community composition under experimental N
621 deposition.

622 Despite the above-described differences in individual compound biochemical
623 composition being distinct under N deposition conditions in the most highly decomposed mineral
624 SOM (Figure 3; Table S7), the biochemical diversity and molecular complexity of mineral SOM
625 as a whole was not altered by N deposition (Figure 5; Figure 6), contradicting our third
626 hypothesis. However, SOM biochemical diversity (i.e., molecular richness and evenness) did
627 change throughout decomposition (Figure 5). Both molecular richness and evenness were higher
628 after one year of decomposition compared to initial undecomposed inputs (Figure 5; Table S17;
629 Table S18). This is likely the result of the production of microbially-derived compounds during
630 the initial phases of root decay. When microbes break down plant litter, new byproducts are
631 produced[7,13,115], which likely explains the observed increases in molecular richness, i.e., the
632 number of compounds present, after one year of decomposition. Molecular richness of mineral
633 SOM returning to the same levels as initial inputs may indicate the complete decay of more
634 accessible components of litter or that the microbially processed C substrates that were produced
635 during one year of decomposition were similarly consumed, returning to the same number of

636 compounds as initial inputs, though the composition of those compounds are distinct (Figure 2;
637 Figure 5). Despite differences in biochemical diversity through decomposition, we did not detect
638 differences in the molecular complexity of SOM between the undecomposed root litter, 1-year
639 decomposed root litter, and mineral SOM (Figure S6; Figure S7). Ultimately these findings
640 indicate that although the composition of the individual compounds changed during decay
641 (Figure 2; Table S5), and were ultimately distinct under N deposition conditions in the most
642 highly decomposed mineral SOM (Figure 2; Figure 3; Table S7), the molecular complexity (i.e.,
643 structural [dis]similarity) of the compounds that constitute SOM at any given stage of
644 decomposition did not (Figure S4). This finding differs from both what has been proposed
645 conceptually about organic matter complexity underlying SOM persistence[15] and from recent
646 studies that have found the opposite: that persistent SOM is less complex than its initial
647 inputs[12,21,116]. In similar studies, SOM persistence was estimated across wider ecosystem ranges
648 (e.g., across soil depths or elevational gradients that span different ecosystem types[12,21,116]) than
649 in this study, which utilized a long-term experiment in sugar maple dominated forests. Thus, in
650 this system, the lack of relationship between SOM molecular complexity and persistence may be
651 attributable to relatively similar site-specific edaphic factors and vegetation composition, which
652 may not be variable enough to detect differences in SOM decay using this method that detects
653 large-scale molecular changes (e.g., terpenes vs. benzenoids). Taken together, our findings
654 suggest that SOM biochemical diversity and molecular complexity are not drivers of SOM
655 persistence in this system.

656 Collectively, our results demonstrate that N deposition altered the abundance of specific
657 compounds in mineral SOM, a reorganization of SOM biochemistry that is not detectable when
658 assessing changes at the less-refined compound class-level, as well as decoupled the relationship

659 between microbial composition and SOM biochemistry. Whether these observed changes have
660 functional implications for the long-term storage of SOM is unknown and warrants further
661 investigation. Though these molecular-level differences in SOM biochemistry under
662 anthropogenic N deposition may appear subtle, the effect that these differences have on the C
663 stored in the system long-term may be disproportionately large. For example, in this system,
664 upon termination of the experimental N deposition, a globally ecologically relevant
665 environmental change in response to Clean Air Act Amendments, microbial activity significantly
666 increased and the C that built up under experimental N deposition was lost from the system
667 within 5-years of treatment termination[40]. Studies have shown that molecular-level changes in
668 SOM biochemistry, in response to various environmental change conditions, impact the capacity
669 of temperate forests to sequester C[117]. A microbial mechanism may underlie this possibility as
670 differences in the structural properties of the molecules in greater abundance under
671 anthropogenic N deposition may have implications for how and by whom these products are
672 transformed, what products are produced, and, ultimately, the decomposability of their
673 byproducts[83,118,119]. Taken together, it is plausible that the SOM that accumulated under
674 experimental N deposition was molecularly distinct as a result of functional changes in the
675 microbial community elicited by the N deposition treatment[24,29]. Thus, upon termination of
676 experimental N deposition, the accumulated, molecularly distinct SOM may have been readily
677 decomposed by the active microbial community upon return to low (i.e., ambient) N conditions.
678 While empirically untested, this response is plausible due to the relative increase in lignin-like
679 compounds, yet observed decrease in the expression of genes that encode lignolytic enzymes[29],
680 as previously observed under experimental N deposition. As such, lignolytic fungal gene
681 expression may rapidly increase in response to reduced N deposition, supporting a rapid decay of

682 the relatively lignin-rich SOM that accumulated during the active experimental N deposition
683 treatment in this long-term study. Future work should explore the relative decomposition
684 potential of different lignin- and lipid-related compounds that were differentially abundant under
685 ambient or the experimental N deposition treatment to deepen our understanding of the potential
686 ecosystem-level consequences of the reorganization of SOM chemistry observed here.

687 **Acknowledgements**

688 We thank Annalisa Stevenson for her help in ArcGIS. We also wish to thank Thea
689 Whitman (and lab), Erika Marín-Spiotta (and lab), and the Department of Soil Science graduate
690 students for their thoughtful feedback on this work.

691 **Funding Declaration**

692 This material is based upon work supported by the National Science Foundation Graduate
693 Research Fellowship Program under Grant No. DGE-2137424 awarded to B.E.P. and from the
694 United States Department of Energy Biological Environmental Research Program. The
695 maintenance of our long-term field experiment is supported by the National Science Foundation
696 Long-Term Research in Environmental Biology Program.

697 **Author Contributions Statement**

698 D.R.Z. designed the study. R.A.U. and W.A.A. performed field and laboratory analyses.
699 A.S.G. performed biochemical analyses. B.E.P. analyzed the data with the help of G.A.C and
700 Z.B.F. B.E.P wrote the first draft of the manuscript. D.R.Z., W.A.A., G.A.C., A.S.G., and Z.B.F.
701 provided significant feedback on subsequent versions and analyses.

References

1. Bowden, R. D. *et al.* Litter Input Controls on Soil Carbon in a Temperate Deciduous Forest. *Soil Sci. Soc. Am. J.* **78**, (2014).
2. Cotrufo, M. F. & Lavallee, J. M. Soil organic matter formation, persistence, and functioning: A synthesis of current understanding to inform its conservation and regeneration. in *Advances in Agronomy* vol. 172 1–66 (Elsevier, 2022).
3. Jenkinson, D. S. & Rayner, J. H. The Turnover of Soil Organic Matter in Some of the Rothamsted Classical Experiments: *Soil Sci.* **123**, 298–305 (1977).
4. Parton, W. J., Schimel, D. S., Cole, C. V. & Ojima, D. S. Analysis of Factors Controlling Soil Organic Matter Levels in Great Plains Grasslands. *Soil Sci. Soc. Am. J.* **51**, 1173–1179 (1987).
5. Adair, E. C. *et al.* Simple three-pool model accurately describes patterns of long-term litter decomposition in diverse climates. *Glob. Change Biol.* **14**, 2636–2660 (2008).
6. Berg, B. & Meentemeyer, V. Litter quality in a north European transect versus carbon storage potential. *Plant Soil* **242**, 83–92 (2002).
7. Cotrufo, M. F., Wallenstein, M. D., Boot, C. M., Denef, K. & Paul, E. The Microbial Efficiency-Matrix Stabilization (MEMS) framework integrates plant litter decomposition with soil organic matter stabilization: do labile plant inputs form stable soil organic matter? *Glob. Change Biol.* **19**, 988–995 (2013).
8. Prescott, C. E. Litter decomposition: what controls it and how can we alter it to sequester more carbon in forest soils? *Biogeochemistry* **101**, 133–149 (2010).
9. Zhang, D., Hui, D., Luo, Y. & Zhou, G. Rates of litter decomposition in terrestrial ecosystems: global patterns and controlling factors. *J. Plant Ecol.* **1**, 85–93 (2008).

10. Berg, B. & McClaugherty, C. *Plant Litter*. (Springer Berlin Heidelberg, Berlin, Heidelberg, 2008). doi:10.1007/978-3-540-74923-3.

11. Waksman, S. A. Humus Origin, Chemical Composition, and Importance in Nature. *Soil Science* **41**, (1936).

12. Jones, A. R. *et al.* Molecular complexity and diversity of persistent soil organic matter. *Soil Biol. Biochem.* **184**, 109061 (2023).

13. Kallenbach, C. M., Frey, S. D. & Grandy, A. S. Direct evidence for microbial-derived soil organic matter formation and its ecophysiological controls. *Nat. Commun.* 10 (2016).

14. Lehmann, J. & Kleber, M. The contentious nature of soil organic matter. *Nature* **528**, 60–68 (2015).

15. Lehmann, J. *et al.* Persistence of soil organic carbon caused by functional complexity. *Nat. Geosci.* **13**, 529–534 (2020).

16. Talbot, J. M., Yelle, D. J., Nowick, J. & Treseder, K. K. Litter decay rates are determined by lignin chemistry. *Biogeochemistry* **108**, 279–295 (2012).

17. Wickings, K., Grandy, A. S., Reed, S. C. & Cleveland, C. C. The origin of litter chemical complexity during decomposition. *Ecol. Lett.* **15**, 1180–1188 (2012).

18. Sugai, S. F. & Schimel, J. P. Decomposition and biomass incorporation of 14c-labeled glucose and phenolics in taiga forest floor: effect of substrate quality, successional state, and season. *Soil Biol. Biochem.* **25**, 1379–1389 (1993).

19. Whalen, E. D. *et al.* Clarifying the evidence for microbial- and plant-derived soil organic matter, and the path toward a more quantitative understanding. *Glob. Change Biol.* gcb.16413 (2022) doi:10.1111/gcb.16413.

20. Angst, G., Mueller, K. E., Nierop, K. G. J. & Simpson, M. J. Plant- or microbial-derived? A review on the molecular composition of stabilized soil organic matter. *Soil Biol. Biochem.* **156**, 108189 (2021).

21. Davenport, R. *et al.* Decomposition decreases molecular diversity and ecosystem similarity of soil organic matter. *Proc. Natl. Acad. Sci.* **120**, e2303335120 (2023).

22. Yang, S. *et al.* Soil organic carbon content and mineralization controlled by the composition, origin and molecular diversity of organic matter: A study in tropical alpine grasslands. *Soil Tillage Res.* **215**, 105203 (2022).

23. Tang, X., Chang, C. & Li, M. Pyrolysis gas chromatography mass spectrometry (py-GC/MS) revealed independent effects of precipitation and temperature on diversity and molecular composition of soil organic matter. *Environ. Earth Sci.* **84**, 164 (2025).

24. Argiroff, W. A., Zak, D. R., Upchurch, R. A., Salley, S. O. & Grandy, A. S. Anthropogenic N deposition alters soil organic matter biochemistry and microbial communities on decaying fine roots. *Glob. Change Biol.* **25**, 4369–4382 (2019).

25. Zak, D. R., Holmes, W. E., Burton, A. J., Pregitzer, K. S. & Talhelm, A. F. Simulated Atmospheric NO_3^- Deposition Increases Soil Organic Matter By Slowing Decomposition. *Ecol. Appl.* **18**, 2016–2027 (2008).

26. Whittinghill, K. A., Currie, W. S., Zak, D. R., Burton, A. J. & Pregitzer, K. S. Anthropogenic N Deposition Increases Soil C Storage by Decreasing the Extent of Litter Decay: Analysis of Field Observations with an Ecosystem Model. *Ecosystems* **15**, 450–461 (2012).

27. Freedman, Z. & Zak, D. R. Atmospheric N Deposition Increases Bacterial Laccase-Like Multicopper Oxidases: Implications for Organic Matter Decay. *Appl. Environ. Microbiol.* **80**, 4460–4468 (2014).

28. Freedman, Z. B., Upchurch, R. A. & Zak, D. R. Microbial Potential for Ecosystem N Loss Is Increased by Experimental N Deposition. *PLOS ONE* **11**, e0164531 (2016).

29. Zak, D. R. *et al.* Anthropogenic N deposition, fungal gene expression, and an increasing soil carbon sink in the Northern Hemisphere. *Ecology* **100**, (2019).

30. Angst, G., Mueller, K. E., Kögel-Knabner, I., Freeman, K. H. & Mueller, C. W. Aggregation controls the stability of lignin and lipids in clay-sized particulate and mineral associated organic matter. *Biogeochemistry* **132**, 307–324 (2017).

31. Bol, R., Poirier, N., Balesdent, J. & Gleixner, G. Molecular turnover time of soil organic matter in particle-size fractions of an arable soil. *Rapid Commun. Mass Spectrom.* **23**, 2551–2558 (2009).

32. Geng, J. *et al.* Different Molecular Characterization of Soil Particulate Fractions under N Deposition in a Subtropical Forest. *Forests* **10**, 914 (2019).

33. Grandy, A. S. & Neff, J. C. Molecular C dynamics downstream: The biochemical decomposition sequence and its impact on soil organic matter structure and function. *Sci. Total Environ.* **404**, 297–307 (2008).

34. Petrén, H., Köllner, T. G. & Junker, R. R. Quantifying chemodiversity considering biochemical and structural properties of compounds with the R package CHEMODIV. *New Phytol.* **237**, 2478–2492 (2023).

35. Burton, A. J., Ramm, C. W., Pregitzer, K. S. & Reed, D. D. Use of multivariate methods in forest research site selection. *Can. J. For. Res.* **21**, 1573–1580 (1991).

36. Jon Dewitz. National Land Cover Database (NLCD) 2019 Products (ver. 3.0, February 2024). U.S. Geological Survey https://doi.org/10.5066/P9KZCM54 (2024).

37. Xia, M., Talhelm, A. F. & Pregitzer, K. S. Long-Term Simulated Atmospheric Nitrogen Deposition Alters Leaf and Fine Root Decomposition. *Ecosystems* **21**, 1–14 (2018).

38. Pregitzer, K. S. *et al.* Fine Root Architecture of Nine North American Trees. *Ecol. Monogr.* **72**, 293–309 (2002).

39. Xia, M., Talhelm, A. F. & Pregitzer, K. S. Fine roots are the dominant source of recalcitrant plant litter in sugar maple-dominated northern hardwood forests. *New Phytol.* **208**, 715–726 (2015).

40. Propson, B. E., Zak, D. R., Classen, A. T., Burton, A. J. & Freedman, Z. B. Gains in soil carbon storage under anthropogenic nitrogen deposition are rapidly lost following its cessation. *Ecology* **105**, e4444 (2024).

41. Rose, R. E. & Bailey, R. W. Ethylene Oxide for Soil Sterilization. *Nature* **169**, 716–716 (1952).

42. Gennari, M., Negre, M. & Ambrosoli, R. Effects of ethylene oxide on soil microbial content and some soil chemical characteristics. *Plant Soil* **102**, 197–200 (1987).

43. Berns, A. E. *et al.* Effect of gamma-sterilization and autoclaving on soil organic matter structure as studied by solid state NMR, UV and fluorescence spectroscopy. *Eur. J. Soil Sci.* **59**, 540–550 (2008).

44. Hobbie, S. E. Contrasting Effects of Substrate and Fertilizer Nitrogen on the Early Stages of Litter Decomposition. *Ecosystems* **8**, 644–656 (2005).

811 45. Grandy, A. S., Strickland, M. S., Lauber, C. L., Bradford, M. A. & Fierer, N. The
812 influence of microbial communities, management, and soil texture on soil organic matter
813 chemistry. *Geoderma* **150**, 278–286 (2009).
814 46. Pold, G., Grandy, A. S., Melillo, J. M. & DeAngelis, K. M. Changes in substrate
815 availability drive carbon cycle response to chronic warming. *Soil Biol. Biochem.* **110**, 68–78
816 (2017).
817 47. Vilgalys, R. & Hester, M. Rapid genetic identification and mapping of enzymatically
818 amplified ribosomal DNA from several Cryptococcus species. *J. Bacteriol.* **172**, 4238–4246
819 (1990).
820 48. Lane, D. J. 16S/23S rRNA sequencing. *Nucleic acid techniques in bacterial systematics*
821 (1991).
822 49. Schloss, P. D. *et al.* Introducing mothur: Open-Source, Platform-Independent,
823 Community-Supported Software for Describing and Comparing Microbial Communities.
824 *Appl. Environ. Microbiol.* **75**, 7537–7541 (2009).
825 50. Mueller, R. C., Balasch, M. M. & Kuske, C. R. Contrasting soil fungal community
826 responses to experimental nitrogen addition using the large subunit rRNA taxonomic marker
827 and cellobiohydrolase I functional marker. *Mol. Ecol.* **23**, 4406–4417 (2014).
828 51. Quast, C. *et al.* The SILVA ribosomal RNA gene database project: improved data
829 processing and web-based tools. *Nucleic Acids Res.* **41**, D590–D596 (2012).
830 52. Cole, J. R. *et al.* Ribosomal Database Project: data and tools for high throughput rRNA
831 analysis. *Nucleic Acids Res.* **42**, D633–D642 (2014).

832 53. Wang, Q., Garrity, G. M., Tiedje, J. M. & Cole, J. R. Naïve Bayesian Classifier for Rapid
833 Assignment of rRNA Sequences into the New Bacterial Taxonomy. *Appl. Environ. Microbiol.*
834 **73**, 5261–5267 (2007).
835 54. Anderson, M. J. PERMANOVA_2factor: a FORTRAN computer program for
836 permutational multivariate analysis of variance (for any two-factor ANOVA design) using
837 permutation tests. *Department of Statistics, University of Auckland, Auckland* 35 (2004).
838 55. Langley, S. R. & Mayr, M. Comparative analysis of statistical methods used for detecting
839 differential expression in label-free mass spectrometry proteomics. *J. Proteomics* **129**, 83–92
840 (2015).
841 56. Yang, L. & Chen, J. A comprehensive evaluation of microbial differential abundance
842 analysis methods: current status and potential solutions. *Microbiome* **10**, 130 (2022).
843 57. Nguyen, N. H. *et al.* FUNGuild: An open annotation tool for parsing fungal community
844 datasets by ecological guild. *Fungal Ecol.* **20**, 241–248 (2016).
845 58. Benjamini, Y. & Hochberg, Y. Controlling the false discovery rate: a practical and
846 powerful approach to multiple testing. *Journal of the Royal statistical society: series B* **57**,
847 289–300 (1995).
848 59. Love, M. I., Huber, W. & Anders, S. Moderated estimation of fold change and dispersion
849 for RNA-seq data with DESeq2. *Genome Biol.* **15**, 550 (2014).
850 60. Oksanen, J. *et al.* vegan: Community Ecology Package. 2.7–1
851 https://doi.org/10.32614/CRAN.package.vegan (2001).
852 61. Pielou, E. C. The measurement of diversity in different types of biological collections. *J.*
853 *Theor. Biol.* **13**, 131–144 (1966).

854 62. Bertz, S. H. The first general index of molecular complexity. *J. Am. Chem. Soc.* **103**,
855 3599–3601 (1981).
856 63. Hendrickson, J. B., Huang, P. & Toczko, A. G. Molecular complexity: a simplified
857 formula adapted to individual atoms. *J. Chem. Inf. Comput. Sci.* **27**, 63–67 (1987).
858 64. Kim, S. *et al.* PubChem 2025 update. *Nucleic Acids Res.* **53**, D1516–D1525 (2025).
859 65. R Core Team. R: A Language and Environment for Statistical Computing. R Foundation
860 for Statistical Computing (2022).
861 66. RStudio Team. RStudio: Integrated development environment for R. (2022).
862 67. Arnhold, E. easyanova: Analysis of Variance and Other Important Complementary
863 Analyses. 11.0 https://doi.org/10.32614/CRAN.package.easyanova (2012).
864 68. Wickham, H. *et al.* Welcome to the Tidyverse. *J. Open Source Softw.* **4**, 1686 (2019).
865 69. Geng, J., Fang, H., Cheng, S. & Pei, J. Effects of N deposition on the quality and quantity
866 of soil organic matter in a boreal forest: Contrasting roles of ammonium and nitrate. *CATENA*
867 **198**, 104996 (2021).
868 70. Sanderman, J. & Grandy, A. S. Ramped thermal analysis for isolating biologically
869 meaningful soil organic matter fractions with distinct residence times. *SOIL* **6**, 131–144
870 (2020).
871 71. Arteaga-Clemente, G., García-González, M. A. & González-González, M. Soil lipid
872 analysis by chromatography: A critical review of the current state in sample preparation. *J.*
873 *Chromatogr. Open* **6**, 100173 (2024).
874 72. Dinel, H., Schnitzer, M. & Mehuys, G. R. Soil Lipids: Origin, Nature, Content,
875 Decomposition, and Effect on Soil Physical Properties. in *Soil Biochemistry* 397–430
876 (Routledge, 2017). doi:10.1201/9780203739389-8.

73. Kindler, R., Miltner, A., Thullner, M., Richnow, H.-H. & Kästner, M. Fate of bacterial biomass derived fatty acids in soil and their contribution to soil organic matter. *Org. Geochem.* **40**, 29–37 (2009).

74. Miltner, A., Bombach, P., Schmidt-Brücken, B. & Kästner, M. SOM genesis: microbial biomass as a significant source. *Biogeochemistry* **111**, 41–55 (2012).

75. Olivelli, M. S. *et al.* Unraveling Mechanisms behind Biomass–Clay Interactions Using Comprehensive Multiphase Nuclear Magnetic Resonance (NMR) Spectroscopy. *ACS Earth Space Chem.* **4**, 2061–2072 (2020).

76. Rempfert, K. R. *et al.* Biomolecular budget of persistent, microbial-derived soil organic carbon: The importance of underexplored pools. *Sci. Total Environ.* **932**, 172916 (2024).

77. Cyle, K. T., Klein, A. R., Aristilde, L. & Martínez, C. E. Ecophysiological Study of *Paraburkholderia* sp. Strain 1N under Soil Solution Conditions: Dynamic Substrate Preferences and Characterization of Carbon Use Efficiency. *Appl. Environ. Microbiol.* **86**, e01851-20 (2020).

78. Stone, B. W. G. *et al.* Life history strategies among soil bacteria—dichotomy for few, continuum for many. *ISME J.* https://doi.org/10.1038/s41396-022-01354-0 (2023) doi:10.1038/s41396-022-01354-0.

79. Khan, K. S., Mack, R., Castillo, X., Kaiser, M. & Joergensen, R. G. Microbial biomass, fungal and bacterial residues, and their relationships to the soil organic matter C/N/P/S ratios. *Geoderma* **271**, 115–123 (2016).

80. Liang, C., Amelung, W., Lehmann, J. & Kästner, M. Quantitative assessment of microbial necromass contribution to soil organic matter. *Glob. Change Biol.* **25**, 3578–3590 (2019).

900 81. Fahy, E. *et al.* Update of the LIPID MAPS comprehensive classification system for
901 lipids. *J. Lipid Res.* **50**, S9–S14 (2009).
902 82. Liebisch, G. *et al.* Update on LIPID MAPS classification, nomenclature, and shorthand
903 notation for MS-derived lipid structures. *J. Lipid Res.* **61**, 1539–1555 (2020).
904 83. Tian, Z. *et al.* PMhub 1.0: a comprehensive plant metabolome database. *Nucleic Acids*
905 *Res.* **52**, D1579–D1587 (2024).
906 84. Klier, K. M. & Anantharaman, K. An updated view of metabolic handoffs in
907 microbiomes. *Trends Microbiol.* S0966842X25002203 (2025) doi:10.1016/j.tim.2025.07.009.
908 85. Harper, D. B. Microbial metabolism of aromatic nitriles. Enzymology of C–N cleavage
909 by *Nocardia* sp. (*Rhodochrous* group) N.C.I.B. 11216. *Biochem. J.* **165**, 309–319 (1977).
910 86. Howden, A. J. M., Rico, A., Mentlak, T., Miguet, L. & Preston, G. M. *Pseudomonas*
911 *syringae* pv. *syringae* B728a hydrolyses indole-3-acetonitrile to the plant hormone indole-3-
912 acetic acid. *Mol. Plant Pathol.* **10**, 857–865 (2009).
913 87. Thimann, K. V. & Mahadevan, S. Nitrilase. *Arch. Biochem. Biophys.* **105**, 133–141
914 (1964).
915 88. Pace, H. C. & Brenner, C. The nitrilase superfamily: classification, structure and
916 function. *Genome Biol.* **2**, reviews0001.1 (2001).
917 89. Bessonnet, T. *et al.* Purification and Characterization of Nitphym, a Robust Thermostable
918 Nitrilase From Paraburkholderia phymatum. *Front. Bioeng. Biotechnol.* **9**, 686362 (2021).
919 90. Moulin, L. *et al.* Complete Genome sequence of Burkholderia phymatum STM815T, a
920 broad host range and efficient nitrogen-fixing symbiont of Mimosa species. *Stand. Genomic*
921 *Sci.* **9**, 763–774 (2014).

922 91. Teepakorn, C. *et al.* Nitrilase immobilization and transposition from a micro-scale batch
923 to a continuous process increase the nicotinic acid productivity. *Biotechnol. J.* **16**, 2100010
924 (2021).
925 92. Vergne-Vaxelaire, C. *et al.* Nitrilase Activity Screening on Structurally Diverse
926 Substrates: Providing Biocatalytic Tools for Organic Synthesis. *Adv. Synth. Catal.* **355**, 1763–
927 1779 (2013).
928 93. Wilhelm, R. C., DeRito, C. M., Shapleigh, J. P., Madsen, E. L. & Buckley, D. H.
929 Phenolic acid-degrading *Paraburkholderia* prime decomposition in forest soil. *ISME*
930 *Commun.* **1**, 4 (2021).
931 94. Bhatnagar, J. M., Peay, K. G. & Treseder, K. K. Litter chemistry influences
932 decomposition through activity of specific microbial functional guilds. *Ecol. Monogr.* **88**,
933 429–444 (2018).
934 95. Pisani, O., Frey, S. D., Simpson, A. J. & Simpson, M. J. Soil warming and nitrogen
935 deposition alter soil organic matter composition at the molecular-level. *Biogeochemistry* **123**,
936 391–409 (2015).
937 96. Thirunavukkarasu, A. *et al.* Unraveling the dynamics of lignin chemistry on
938 decomposition to understand its contribution to soil organic matter accumulation. *Plant Soil*
939 https://doi.org/10.1007/s11104-024-07066-y (2024) doi:10.1007/s11104-024-07066-y.
940 97. vandenEnden, L. *et al.* Molecular-level changes in soil organic matter composition after
941 10 years of litter, root and nitrogen manipulation in a temperate forest. *Biogeochemistry* **141**,
942 183–197 (2018).
943 98. Alruwaili, A. *et al.* Elucidation of microbial lignin degradation pathways using synthetic
944 isotope-labelled lignin. *RSC Chem. Biol.* **4**, 47–55 (2023).

945 99. DeAngelis, K. M. *et al.* Characterization of Trapped Lignin-Degrading Microbes in
946 Tropical Forest Soil. *PLoS ONE* **6**, e19306 (2011).
947 100. DeAngelis, K. M. *et al.* Evidence supporting dissimilatory and assimilatory lignin
948 degradation in Enterobacter lignolyticus SCF1. *Front. Microbiol.* **4**, (2013).
949 101. Bugg, T. D. H., Ahmad, M., Hardiman, E. M. & Rahmanpour, R. Pathways for
950 degradation of lignin in bacteria and fungi. *Nat. Prod. Rep.* **28**, 1883 (2011).
951 102. Janusz, G. *et al.* Lignin degradation: microorganisms, enzymes involved, genomes
952 analysis and evolution. *FEMS Microbiol. Rev.* **41**, 941–962 (2017).
953 103. Lee, S., Kang, M., Bae, J.-H., Sohn, J.-H. & Sung, B. H. Bacterial Valorization of Lignin:
954 Strains, Enzymes, Conversion Pathways, Biosensors, and Perspectives. *Front. Bioeng.*
955 *Biotechnol.* **7**, 209 (2019).
956 104. Bugg, T. D., Ahmad, M., Hardiman, E. M. & Singh, R. The emerging role for bacteria in
957 lignin degradation and bio-product formation. *Curr. Opin. Biotechnol.* **22**, 394–400 (2011).
958 105. Granja-Travez, R. S., Persinoti, G. F., Squina, F. M. & Bugg, T. D. H. Functional
959 genomic analysis of bacterial lignin degraders: diversity in mechanisms of lignin oxidation
960 and metabolism. *Appl. Microbiol. Biotechnol.* **104**, 3305–3320 (2020).
961 106. Gu, J. *et al.* Bacterial transformation of lignin: key enzymes and high-value products.
962 *Biotechnol. Biofuels Bioprod.* **17**, 2 (2024).
963 107. Kim, D., Kim, H.-W., & Hyoungseok Lee. Kraft Lignin Decomposition by Forest Soil
964 Bacterium *Pseudomonas kribbensis* CHA-19. *J. Microbiol. Biotechnol.* **34**, 1867–1875
965 (2024).

108. Ookawa, Z. *et al.* Catabolic System of Syringic Acid, a Key Intermediate of Lignin-Derived Aromatic Compounds, via a Novel Linear Pathway in *Pseudomonas* sp. NGC7. *J. Agric. Food Chem.* **73**, 18899–18913 (2025).

109. Frey, S. D., Knorr, M., Parrent, J. L. & Simpson, R. T. Chronic nitrogen enrichment affects the structure and function of the soil microbial community in temperate hardwood and pine forests. *For. Ecol. Manag.* **196**, 159–171 (2004).

110. Hesse, C. N. *et al.* Forest floor community metatranscriptomes identify fungal and bacterial responses to N deposition in two maple forests. *Front. Microbiol.* **6**, (2015).

111. Li, X. *et al.* Nitrogen addition restricts key soil ecological enzymes and nutrients by reducing microbial abundance and diversity. *Sci. Rep.* **15**, 5560 (2025).

112. Moore, J. A. M. *et al.* Fungal community structure and function shifts with atmospheric nitrogen deposition. *Glob. Change Biol.* **27**, 1349–1364 (2021).

113. Frey, S. D. *et al.* Chronic nitrogen additions suppress decomposition and sequester soil carbon in temperate forests. *Biogeochemistry* **121**, 305–316 (2014).

114. Van Diepen, L. T. A., Frey, S. D., Landis, E. A., Morrison, E. W. & Pringle, A. Fungi exposed to chronic nitrogen enrichment are less able to decay leaf litter. *Ecology* **98**, 5–11 (2017).

115. Prescott, C. E. & Vesterdal, L. Decomposition and transformations along the continuum from litter to soil organic matter in forest soils. *For. Ecol. Manag.* **498**, 119522 (2021).

116. Zhang, Z. *et al.* Changes in molecular composition, diversity, and network complexity of soil organic carbon along the elevation in Changbai Mountain, Northeast China. *Geoderma* **443**, 116842 (2024).

988 117. Castañeda-Gómez, L. *et al.* Soil organic matter molecular composition with long-term
989 detrital alterations is controlled by site-specific forest properties. *Glob. Change Biol.*
990 gcb.16456 (2022) doi:10.1111/gcb.16456.
991 118. Bossio, D. A. *et al.* The role of soil carbon in natural climate solutions. *Nat. Sustain.* **3**,
992 391–398 (2020).
993 119. Crow, S. E. *et al.* Sources of plant-derived carbon and stability of organic matter in soil:
994 implications for global change. *Glob. Change Biol.* **15**, 2003–2019 (2009).
995